



Contents lists available at ScienceDirect

Saudi Journal of Biological Sciences

journal homepage: www.sciencedirect.com

Original article

Cholinesterase inhibitory activity of highly functionalized fluorinated spiropyrrolidine heterocyclic hybrids

Raju Suresh Kumar^{a,*}, Abdulrahman I. Almansour^a, Natarajan Arumugam^a, D. Kotresha^b, Thota Sai Manohar^c, S. Venketesh^c^a Department of Chemistry, College of Science, King Saud University, P.O. Box 2455, Riyadh 11451, Saudi Arabia^b Department of Studies in Botany, Davangere University, Shivagangothri, Davangere 577007, Karnataka, India^c Department of Biosciences, Sri Sathya Sai Institute of Higher Learning, Prasanthi Nilayam, A.P 515 134, India

ARTICLE INFO

Article history:

Received 21 September 2020

Revised 25 October 2020

Accepted 1 November 2020

Available online 11 November 2020

Keywords:

Cholinesterase inhibitory activity

Alzheimer's disease

AChE

BChE

Fluorinated spiroheterocyclic hybrids

Molecular docking simulation

ABSTRACT

Two series of dimethoxyindanone imbedded novel fluorinated spiropyrrolidine heterocyclic hybrids were synthesized employing two different less explored azomethine ylides and were measured for their efficiency as inhibitors for Alzheimer's disease. Among the spiropyrrolidine heterocyclic hybrids, the indole based fluorinated compound with a methoxy substituent at the *meta*- position of the aryl ring exhibited the utmost potent AChE and BChE inhibitory activities with an IC₅₀ of 1.97 ± 0.19 μM and 7.08 ± 0.20 μM respectively. The plausible mechanism of inhibition on ChE receptors was unveiled via molecular docking studies.

© 2020 The Authors. Published by Elsevier B.V. on behalf of King Saud University. This is an open access article under the CC BY-NC-ND license (<http://creativecommons.org/licenses/by-nc-nd/4.0/>).

1. Introduction

Alzheimer's disease (AD) is a major and increasing global health challenge, the dominant reason for dementia, is an irreversible memory linked neurodegenerative illness categorized by developing weakening of memory and perception (Terry & Buccafusco, 2003). AD projected it the 5th leading cause of global deaths. WHO recognizes dementia as a public health priority, it is estimated global incidence around 50 million cases with a dementia accounts for 60–70% living in low and middle-income countries. It is estimated that total number of people with dementia will reach 82 million in 2030 and 152 million in 2050, whereas this scenario is estimated to increase twofold every 20 years (WHO, 2017, 2019). Based on the cholinergic hypothesis, one of the major prominent therapeutic approach to boost cholinergic function is by administering cholinesterase inhibitors (Cumings, 2004).

Two ChEs viz. acetylcholinesterase (AChE) and butyrylcholinesterase (BChE) are accountable for degradation and regulates ACh in human body and therefore dual inhibitors are treasured and beneficial compounds in AD therapy (Genc et al., 2016; Topal et al., 2017). Existing clinically accepted treatments for AD are restricted to cholinesterase inhibitors (ChEI's), working through the inhibition of cholinesterases by hydrolyzing Ach. Limitations of the currently available ChEIs such as short bioavailability and half-lives, slim therapeutic value led us to the unearth novel drug entrants as ChEIs with greater effectiveness and reduced toxicity.

In this perception, heterocyclic hybrids with spiro rings are very fascinating structural motifs for drug discovery as these three-dimensional structures enable communications with three-dimensional binding sites with no difficulty compared to the planar aromatic ring system as ligand. Spiro compounds present in natural products were found to interrelate more proficiently with binding pockets in proteins and were found to have better solubility, a vital property in the development of drugs (Zheng & Tice, 2016). Fluorine is one of the highly active element and is commonly employed in drugs (Champagne et al., 2015; Wilcken et al., 2013). Incorporation of fluorine into bioactive molecules expands its drug-like properties by hindering undesired metabolism at a definite site and ultimately improves the bioavailability.

* Corresponding author.

E-mail address: sraju@ksu.edu.sa (R.S. Kumar).

Peer review under responsibility of King Saud University.



Production and hosting by Elsevier

<https://doi.org/10.1016/j.sjbs.2020.11.005>

1319-562X/© 2020 The Authors. Published by Elsevier B.V. on behalf of King Saud University.

This is an open access article under the CC BY-NC-ND license (<http://creativecommons.org/licenses/by-nc-nd/4.0/>).

More than 20% of the presently available drugs comprise fluorine atoms and consequently, derivatization of active molecules to fluorinated analogues is a prominent strategy to attain potent drug like molecules in drug discovery (Jasem et al., 2016; Wang et al., 2014). In an effort to improve the cholinesterase inhibitory activity of spiro pyrrolidine analogues of our interest, in the present study, we have designed and synthesized a library of fluorine embedded spiro pyrrolidine heterocyclic hybrids and assessed for their cholinesterase inhibitory activity.

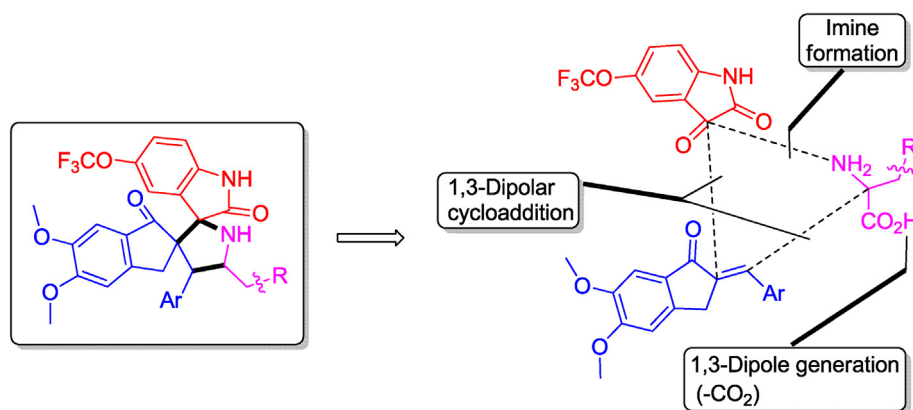
The rising death rate and the abridged therapeutic potential of the presently accessible options to treat AD in coincidence with our sustained interest in the construction of novel drug like spiro heterocycles (Almansour et al., 2020; Kia et al., 2013a; Kia et al., 2013b; Kia et al., 2014a; Kia et al., 2014b; Kia et al., 2014c; Basiri et al., 2013a; Basiri et al., 2013b; Basiri et al., 2014; Kumar et al., 2014a), prompted us in the present work to report a sustainable synthesis of some new fluorinated spiro heterocyclic hybrids and their cholinesterase inhibitory activity. Particularly, the high potency of the spiro pyrrolidine heterocyclic hybrids reported by us (Kumar et al., 2014b; Kumar et al., 2018; Almansour et al., 2015) prompted us to focus our attention towards their fluorinated analogs. As the molecular docking simulation plays a vital part in drug design and employed in visualizing the bonding affinity and total binding energy of heterocyclic drug candidates to the active

site of their target enzymes (Kitchen et al., 2004), we performed the molecular docking simulation of the most active fluorinated analog to reveal its binding interaction mechanisms at the active site of AChE and BChE. Synthetic strategy employed in the present work for the formation of fluorinated spiroheterocyclic hybrids is summarized in scheme 1.

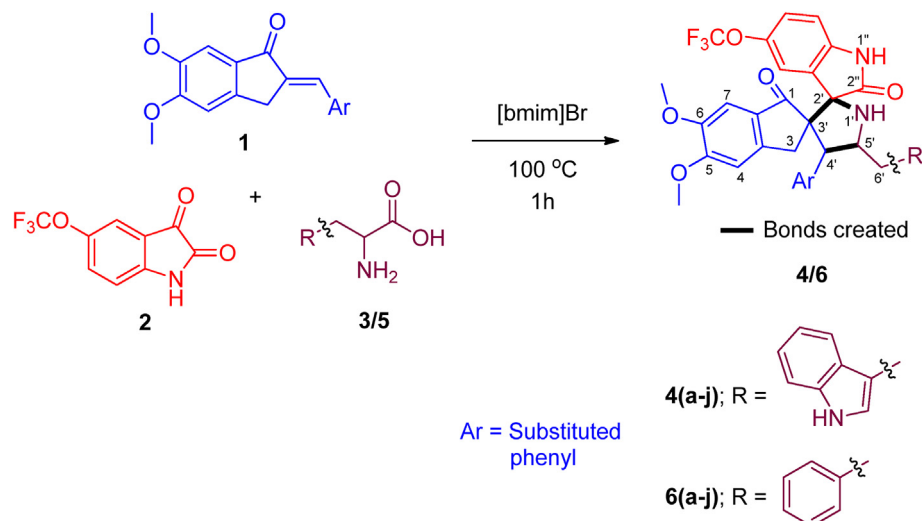
2. Materials and methods

2.1. General experimental procedure for the construction of spiro pyrrolidine heterocyclic hybrids 4/6(a–j)

A mixture of arylmethylidenedimethoxyindenone **1** (1 mmol), trifluoromethoxy isatin **2** (1 mmol), and tryptophan/phenylalanine **3/5** (1 mmol) in 1-Butyl-3-methylimidazolium bromide ([bmim] Br) (200 mg) was heated with stirring at 100 °C for 1 h. The reaction progress and completion were assessed by TLC analysis. Then 10 mL of ethyl acetate was added and the mixture was allowed to stir for 15 min. The solvent phase was separated, washed repeatedly with water, and dried. Column chromatography was used to further purify the spiro pyrrolidine heterocyclic hybrids employing ethyl acetate and petroleum ether (2:3 v/v) as eluent. The ionic liquid [bmim]Br used in the reaction was completely dried under vacuum and recycled for successive reactions.



Scheme 1. Retro synthetic approach employed in the present work.



Scheme 2. Synthesis of fluorinated spiro pyrrolidines 4/6(a–j).

2.2. Physical and characterization data of representative compounds

2.2.1. Spiropyrrolidine heterocyclic hybrid, 4b

White solid, (80%); mp = 163–165 °C; IR (KBr) ν_{\max} 3380, 2935, 1726, 1684, 1618, 1585 cm^{-1} . $^1\text{H NMR}$ (CDCl_3 , 500 MHz): δ_{H} 1.97 (s, 3H, CH_3), 2.64 (d, $J = 18.5$ Hz, 1H, 3- CH_2), 2.76 (d, $J = 18.0$ Hz, 1H, 3- CH_2), 3.02–3.06 (m, 1H, 6'- CH_2), 3.13–3.18 (m, 1H, 6'- CH_2), 3.74 (s, 3H, OCH_3), 3.78 (s, 3H, OCH_3), 4.22 (d, 1H, $J = 9.5$ Hz, H-4'), 5.08–5.11 (m, 1H, H-5'), 6.41 (s, 1H, Ar-H), 6.45 (d, 1H, $J = 8.0$ Hz, Ar-H), 6.76–6.84 (m, 2H, Ar-H), 6.91–7.39 (m, 7H, Ar-H), 7.49 (d, 1H, $J = 8.0$ Hz, Ar-H), 8.01 (d, 1H, $J = 8.0$ Hz, Ar-H), 8.06 (s, 1H, Ar-H), 8.45 (s, 1H, Ar-H). $^{13}\text{C NMR}$ (CDCl_3 , 125 MHz): δ_{C} 20.42, 31.74, 35.14, 55.79, 56.01, 56.12, 64.44, 66.99, 74.97, 104.07, 106.57, 109.98, 112.92, 113.10, 118.47, 119.22, 120.46, 121.79, 122.53, 122.60, 125.97, 126.36, 127.28, 129.14, 130.28, 131.33, 136.18, 138.08, 139.05, 139.71, 145.40, 147.90, 149.40, 155.45, 155.67, 159.29, 179.79, 206.70. Anal. calc. for $\text{C}_{38}\text{H}_{32}\text{F}_3\text{N}_3\text{O}_5$: C, 68.36; H, 4.83; N, 6.29. Found: C, 68.53; H, 4.71; N, 6.40%.

2.2.2. Spiropyrrolidine heterocyclic hybrid, 6b

White solid, (89%); mp = 148–150 °C; IR (KBr) ν_{\max} 3425, 1723, 1685, 1615, 1593 cm^{-1} ; $^1\text{H NMR}$ (CDCl_3 , 500 MHz): δ_{H} 1.81 (brs, 1H, NH), 1.97 (s, 3H, CH_3), 2.60 (d, $J = 18.5$ Hz, 1H, 3- CH_2), 2.75 (d, $J = 18.0$ Hz, 1H, 3- CH_2), 2.89 (dd, $J = 14.0, 9.0$ Hz, 1H, 6'- CH_2), 3.01 (dd, $J = 14.0, 4.0$ Hz, 1H, 6'- CH_2), 3.75 (s, 3H, OCH_3), 3.78 (s, 3H, OCH_3), 4.13 (d, $J = 9.0$ Hz, 1H, H-4'), 4.91–4.95 (m, 1H, H-5'), 6.40 (s, 1H, Ar-H), 6.48 (d, 1H, $J = 8.5$ Hz, Ar-H), 6.84–6.86 (m, 1H, Ar-H), 6.90 (s, 1H, Ar-H), 7.02 (d, 1H, $J = 7.0$ Hz, Ar-H), 7.08–7.12 (m, 2H, Ar-H), 7.18–7.27 (m, 5H, Ar-H), 7.94 (d, 1H, $J = 7.5$ Hz, Ar-H), 8.19 (s, 1H, NH). $^{13}\text{C NMR}$ (CDCl_3 , 125 MHz): δ_{C} 20.39, 35.17, 40.42, 54.39, 55.80, 56.02, 65.13, 66.98, 74.90, 104.07, 106.48, 109.71, 120.59, 122.55, 126.21, 126.34, 126.66, 127.32, 128.31, 128.51, 128.92, 129.45, 130.19, 137.30, 137.92, 138.95, 139.64, 144.26, 147.81, 149.36, 155.58, 179.60, 206.50. Anal. calc. for $\text{C}_{36}\text{H}_{31}\text{F}_3\text{N}_2\text{O}_5$: C, 68.78; H, 4.97; N, 4.46. Found: C, 68.94; H, 4.85; N, 4.57%.

Materials, methods and complete experimental details can be found in the “Supplementary data” section.

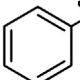
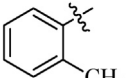
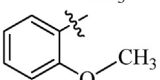
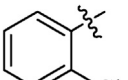
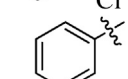
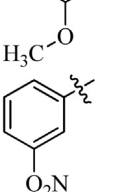
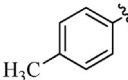
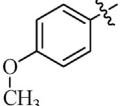
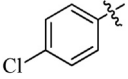
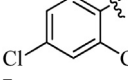
Table 1
Cholinesterase inhibitory activities of 4(a–j).

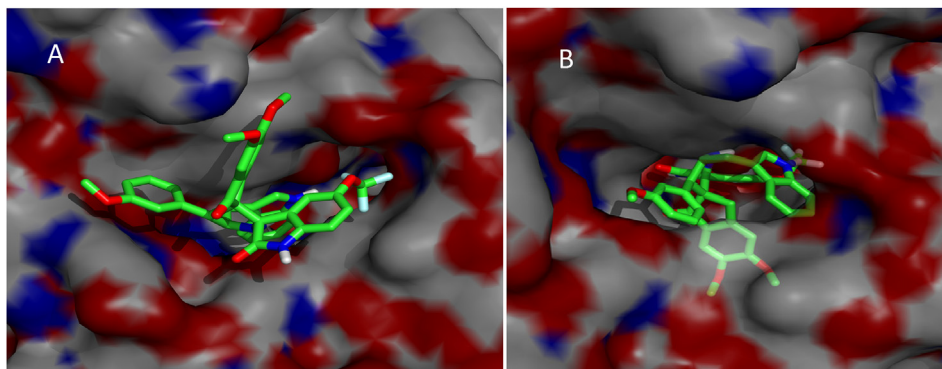
Entry	Ar	Comp	AChE inhibition IC_{50} μM ($\pm\text{SD}$)	BChE inhibition IC_{50} μM ($\pm\text{SD}$)	AChE ^a selectivity	BChE ^b selectivity
1		4a	5.94 \pm 0.12	8.41 \pm 0.15	1.42	0.71
2		4b	6.43 \pm 0.09	8.51 \pm 0.18	1.10	0.91
3		4c	2.48 \pm 0.22	18.36 \pm 0.09	7.40	0.14
4		4d	9.12 \pm 0.18	13.25 \pm 0.16	1.45	0.69
5		4e	1.97 \pm 0.19	7.08 \pm 0.20	4.32	0.23
6		4f	2.54 \pm 0.10	19.40 \pm 25	7.64	0.13
7		4g	12.78 \pm 0.15	9.40 \pm 0.23	0.74	1.36
8		4h	3.46 \pm 0.20	7.12 \pm 0.20	2.06	0.49
9		4i	7.22 \pm 0.26	21.05 \pm 0.16	2.92	0.34
10		4j	14.35 \pm 0.14	11.08 \pm 0.23	0.77	1.30
11	-	Galanthamine	2.08 \pm 0.12	19.24 \pm 0.11	9.25	0.11

^a AChE Selectivity = $\text{IC}_{50}(\text{BChE})/\text{IC}_{50}(\text{AChE})$.

^b BChE Selectivity = $\text{IC}_{50}(\text{AChE})/\text{IC}_{50}(\text{BChE})$.

Table 2
Cholinesterase inhibitory activities of **6(a-j)**.

Entry	Ar	Comp	AChE inhibition IC ₅₀ μM (±SD)	BChE inhibition IC ₅₀ μM (±SD)	AChE ^a selectivity	BChE ^b selectivity
1		6a	10.62 ± 0.17	17.22 ± 0.12	1.62	0.62
2		6b	12.50 ± 0.15	19.43 ± 0.20	1.55	0.64
3		6c	6.41 ± 0.10	12.72 ± 0.11	1.35	0.74
4		6d	17.14 ± 0.20	14.51 ± 0.12	0.85	1.18
5		6e	2.06 ± 0.21	18.50 ± 0.14	8.98	0.11
6		6f	2.21 ± 0.18	14.09 ± 0.15	6.38	0.16
7		6g	10.65 ± 0.20	12.17 ± 0.15	1.14	0.88
8		6h	3.24 ± 0.18	18.05 ± 0.09	5.57	0.18
9		6i	11.32 ± 0.09	17.68 ± 0.24	1.56	0.64
10		6j	8.49 ± 0.16	15.12 ± 0.21	1.78	0.56
11	-	Galanthamine	2.08 ± 0.12	19.24 ± 0.11	9.25	0.11

^a AChE Selectivity = IC₅₀(BChE)/IC₅₀(AChE).^b BChE Selectivity = IC₅₀(AChE)/IC₅₀(BChE).**Fig. 1.** (A and B) Peripheral anionic site and catalytic active site of hAChE displaying **4e**.

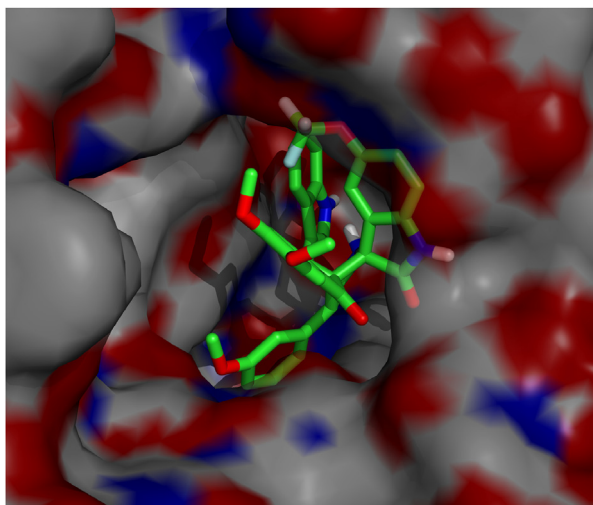


Fig. 2. Active site of hBChE displaying **4e** in the binding pocket of enzyme.

3. Results

The starting substrates 2-arylmethylidene-5,6-dimethoxyindones **1(a-j)** required for the construction of fluorinated spiroheterocyclic hybrids **4/6(a-j)** were synthesized following the literature procedure (Ali et al., 2009). The synthetic procedure adopted for the construction of fluorinated spiroheterocyclic hybrids was shown in scheme 2 and the reaction condition optimized in our previous studies was employed (Almansour et al., 2015). The one pot three-component cycloaddition reaction of 2-arylmethylidene-5,6-dimethoxyindones **1(a-j)** with azomethine ylides generated insitu from 5-fluoroisatin and tryptophan/phenylalanine in [bmim]Br furnished the spiropyrrolidine heterocyclic hybrids **4/6(a-j)** in moderate to good yields. These two series of spiropyrrolidine heterocyclic hybrids **4/6(a-j)** derived using tryptophan and phenylalanine respectively were evaluated in vitro for their ChEI activity against AChE and BChE and the results are described in Tables 1 and 2.

4. Discussion

4.1. Chemistry

In a typical reaction, an equimolar mixture of **1b**, fluoroisatin and tryptophan in [bmim]Br at 100 °C was heated with continuous stirring to afford the fluorinated spiroheterocyclic hybrid good yield (80%). The other spiropyrrolidines of this series employing differently substituted dipolarophiles were also obtained in good yields (76–86%). Similarly, the same synthetic procedure was

applied for the synthesis of analogues of spiropyrrolidines employing the azomethine ylide derived from 5-fluoroisatin and phenylalanine. It is pertinent to mention that the reaction progressed regio and stereoselectively in [bmim]Br, producing only the diastereoisomer **4/6** in racemic form even with the existence of multiple stereocenters. It is also significant to mention that these cycloaddition reactions progressed well irrespective of the steric or electronic properties of the structural sub-units substituted on the aromatic ring of **1**.

Structural interpretation of the spiropyrrolidine heterocyclic hybrids **4/6(a-j)** was performed using spectroscopic techniques. Structural interpretation of these compounds was derived by considering a representative example **6b**. A singlet at δ 1.97 ppm is readily assigned to the methyl group of the aryl ring whereas the other two singlets at δ 3.75 ppm and 3.78 ppm were due to the methoxy group substituted at dimethoxyindanone ring. The doublet at δ 2.60 ppm with $J = 18.5$ Hz is due to one of the 3-CH₂ proton of the dimethoxyindanone ring. H,H-COSY correlation of this proton with the other doublet at δ 2.75 ppm is associated to the remaining proton of 3-CH₂. The two doublet of doublets at 2.89 ppm and 3.01 ppm were attributed to 6'-CH₂. The doublet at 4.13 ppm and the multiplet at 4.91–4.95 ppm were assigned to H-4' and H-5' respectively. The singlets, doublets and multiplets around 6.40–8.19 ppm were due to the aromatic protons. In the ¹³C NMR spectrum, the presence of nine carbon signals in the aliphatic region confirms the presence of –CH₃, –OCH₃, –CH, –CH₂ and spiro carbons. The signals at 179.60 ppm and 206.50 ppm were due to the carbonyl carbons whilst the aromatic carbons resonated between 104.07 ppm and 155.58 ppm. The structure of other heterocyclic hybrids was also derived by similar considerations. The fluorinated spiropyrrolidines **4/6(a-j)** are formed through a mechanistic pathway as reported by us for analogues compounds involving the creation of two new C–C and one C–N bonds (Kumar et al., 2014a; Kumar et al., 2018; Almansour et al., 2015). [Bmim]Br play dual roles, both as a green solvent and catalyst in these cycloaddition reactions affording the cycloadducts **4/6(a-j)** regio- and stereoselectively in moderate to good yields.

4.2. Biology

All the spiropyrrolidine heterocyclic hybrids embedded with indole subunit **4(a-j)**, displayed moderate to good AChE inhibitory activities (Table 1). Among them, four compounds namely **4c**, **4e**, **4f** and **4h** with IC₅₀ 2.48 ± 0.22, 1.97 ± 0.19, 2.54 ± 0.10 and 3.46 ± 0.20 μM showed comparable activity with the standard drug galanthamine with IC₅₀ of 2.08 ± 0.12 μM. Furthermore, compounds **4a**, **4b**, **4d** and **4i** displayed activity <10 μM and compounds **4g** and **4j** displayed activity with IC₅₀ 12.78 ± 0.15 and 14.35 ± 0.14 μM. It is appropriate to note from table 1 that the compounds with methoxy substituent at different positions of

Table 3
Amino acid residues in the binding pockets of hAChE and hBChE interacting with compound **4e**.

Compound	Protein	Binding Energy (Kcal/mol)	Amino acids involved in Interactions
4e	hAChE (peripheral anionic site)	–10.5	Hydrophobic Interactions: Tyr72, Asp74, Leu76, Trp286, Leu289, Gln291, Glu292, Ser293, Phe295, Gly342 Hydrogen Bonding: His287 (bond length, 3.23) Tyr341 (bond length, 2.93)
4e	hAChE (catalytic active site)	6.9	Hydrophobic Interactions: Asp74, Gly82, Thr83, Gly120, Gly121, Gly122, Tyr124, Gly126, Leu130, Tyr133, Glu202, Phe295, Phe297, Tyr337, Phe338, Tyr341, Trp439, Pro446, Hydrogen Bonding: Trp86(bond length, 1.95); Ser125(bond length, 2.88); Ser203(bond length, 2.92); Tyr449 (bond length, 2.75) His447 has ligand bond with 4e
4e	hBChE	–11.0	Hydrophobic Interactions: Ile69, Asp70, Ser79, Trp82, Asn83, Gly115, Gly116, Gly117, Thr120, Leu125, Glu197, Ser198, Leu286, Ser287, Val288, Ala328, Phe329, Trp332, Phe398, His438 Hydrogen Bonding: Tyr128 (bond length, 3.22)

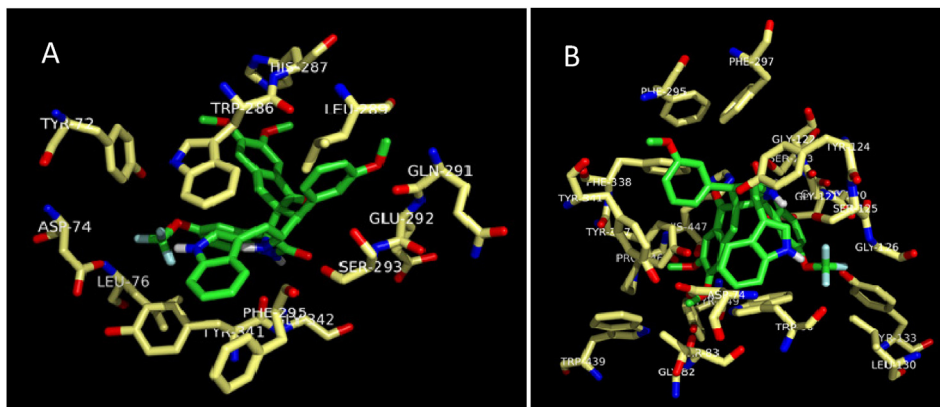


Fig. 3. (A and B) Amino acid residues of hAChE involved in the hydrogen and hydrophobic interactions with **4e** at Peripheral anionic and catalytic active sites.

the aryl subunit at C-4' of the pyrrolidine ring displayed the most potent activity among other analogues. Whereas all these synthesized compounds displayed comparable BChE inhibitory activities ranging from 7.08 ± 0.20 to 21.05 ± 0.16 μM when compared to the standard drug galanthamine with IC_{50} of 19.24 ± 0.11 μM . It

is noteworthy to mention that the most active compound being the same as in AChE, the meta methoxy substituted analogue, **4e**. Over-all, as stated in our earlier report (Kumar et al., 2014a), among the spiropyrrrolidine heterocyclic hybrids **4(a-j)**, compounds with ortho- and meta substituents at the aryl ring displayed enhanced inhibition compared to para-substituted aryl rings (Table 1).

The spiropyrrrolidine heterocyclic hybrids **6(a-j)** with phenyl subunit also displayed good ChEI activities but with a less magnitude compared to their indole analogues **4(a-j)**. AChE inhibitory activities of the series **6(a-j)** ranges from IC_{50} 2.06 ± 0.21 to 17.14 ± 0.20 μM (Table 2). The highest AChE inhibitory activity was recorded for compound **6e** with IC_{50} 2.06 ± 0.21 μM followed by the compound **6f** with meta- nitro substituted aryl ring with an IC_{50} of 2.21 ± 0.18 μM . Compounds **6h** and **6c** are the subsequent potent compounds of the series with IC_{50} of 3.24 ± 0.18 μM and 6.41 ± 0.10 μM . Other compounds of the series viz, **6a**, **6b**, **6d**, **6g** and **6i** showed $\text{IC}_{50} > 10$ μM while compound **6j** possessed an IC_{50} of 8.49 ± 0.16 μM . As mentioned earlier, the compounds with methoxy substituents showed predominant AChE inhibitory activity when compared to other compounds of the series. All the compounds, **6(a-j)** of the series displayed notable BChE inhibitory activity with IC_{50} ranging from 12.17 ± 0.15 μM to 19.43 ± 0.20 μM . In general, the spiropyrrrolidine heterocyclic hybrids **4(a-j)** with indole subunit displayed comparably better ChEI activity than the hybrids with phenyl units **6(a-j)**.

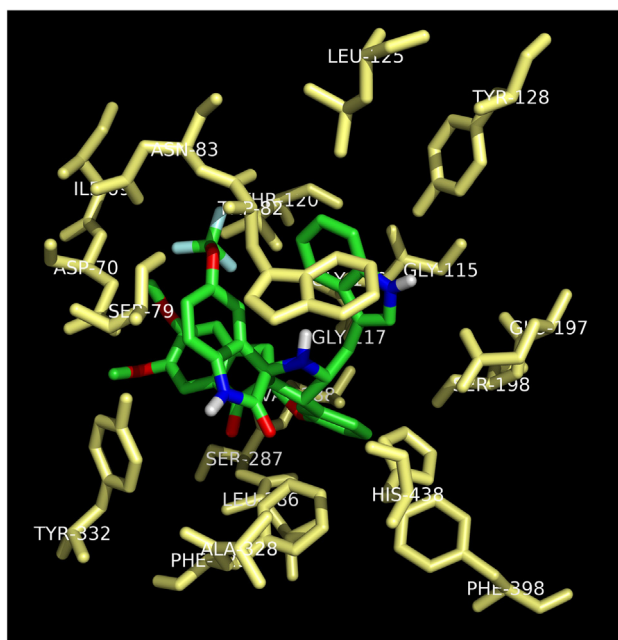


Fig. 4. Amino acid residues of hBChE involved in the hydrogen and hydrophobic interactions with **4e**.

4.3. Molecular docking simulation

The most active compound, meta methoxy substituted spiropyrrrolidine heterocyclic hybrid **4e**, is selected for docking simulations

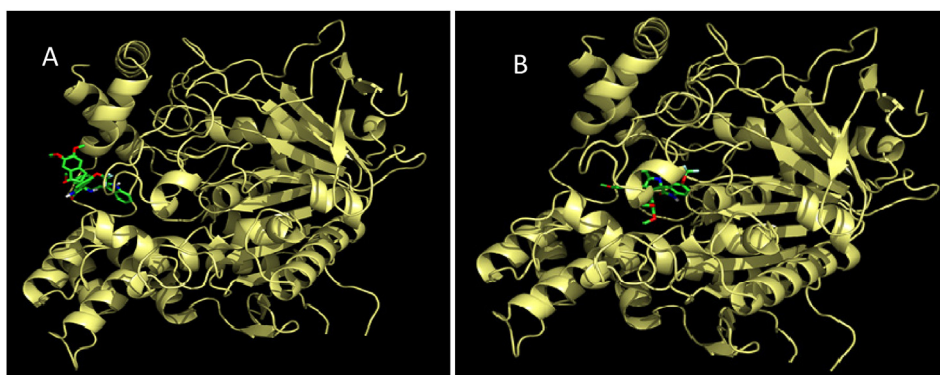


Fig. 5. (A and B) Cartoon view of hAChE with **4e**, at the peripheral anionic and catalytic active sites.



Fig. 6. Cartoon view of hBChE with 4e.

using *AutoDock/Vina* (Trott & Olson, 2010) plugin for PyMOL. The affinity of compound 4e to hAChE is higher with the peripheral anionic site (PAS) (binding energy: -10.5 Kcal/mol) than the catalytic active site (CAS) (binding energy: 6.9 Kcal/mol). At the PAS, compound 4e formed 10 hydrophobic interactions and 1 hydrogen bond with hAChE. At the CAS, though it formed 18 hydrophobic interactions and 4 hydrogen bonds, His447 formed a ligand bond with 4e. The binding affinity of compound 4e with hBChE is found to be better with a binding energy of -11.0 Kcal/mol compared to hAChE. 4e formed 20 hydrophobic interactions and 1 hydrogen bond with hBChE. The docked 4e in the PAS and CAS of hAChE are depicted in Fig. 1A and Fig. 1B and with hBChE in Fig. 2. The compound 4e represented as sticks, is docked in the active site of the two cholinesterases shown in surface view and the Table 3 summarizes the binding energies (Kcal/mol) and the interacting amino acid residues of hAChE at PAS (Fig. 3A) and CAS (Fig. 3B) and the amino acid residues of hBChE, interacting with the compound 4e (Fig. 4). The ribbon view of the two cholinesterases with 4e docked at the PAS and CAS of hAChE and hBChE are shown in Fig. 5A and Fig. 5B and Fig. 6, respectively.

To evaluate the physicochemical properties and assess the absorption, distribution, metabolism and excretion (ADME) of compound 4e, we used the Swiss ADME web tool (Daina et al., 2017) (<http://www.swissadme.ch>) and summarized some of these important properties of compound 4e in Table S1 (vide supplementary data).

5. Conclusions

Two series of fluorine impregnated spiropyrrolidine heterocyclic hybrids were synthesized through a three-component cycloaddition reaction of less explored azomethine ylides generated *in situ* from trifluoromethoxyisatin and tryptophan/phenylalanine with 2-arylmethylidene-5,6-dimethoxyindenes in good yields employing [bmim]Br as the green solvent. Both series of compounds exhibited promising AChE and BChE inhibitory activities, the spiropyrrolidine heterocyclic hybrids with indole subunit displayed comparably better ChEI activity than the heterocyclic hybrids with phenyl units. It is noteworthy to mention that the compounds with methoxy substituted aryl ring displayed IC_{50} val-

ues comparable with that of the standard drug galanthamine, molecular docking studies of this compound disclosed good correlations between IC_{50} values and free binding energy.

Declaration of Competing Interest

The authors declare that they have no known competing financial interests or personal relationships that could have appeared to influence the work reported in this paper.

Acknowledgement

This project was supported by Researchers Supporting Project number (RSP-2020/231), King Saud University, Riyadh, Saudi Arabia.

Appendix A. Supplementary material

Supplementary data to this article can be found online at <https://doi.org/10.1016/j.sjbs.2020.11.005>.

References

- Ali, M.A., Yar, M.S., Hasan, M.Z., Ahsan, M.J., Pandian, S., 2009. Design, synthesis and evaluation of novel 5,6-dimethoxy-1-oxo-2,3-dihydro-1H-2-indenyl-3,4-substituted phenyl methanone analogues. *Bioorg. Med. Chem. Lett.* 19, 5075–5077.
- Almansour, A.I., Arumugam, N., Kumar, R.S., Kotresha, D., Manohar, T.S., Venketesh, S., 2020. Design, synthesis and cholinesterase inhibitory activity of novel spiropyrrolidine tethered imidazole heterocyclic hybrid. *Bioorg. Med. Chem. Lett.* 30, 126789.
- Almansour, A.I., Kumar, R.S., Arumugam, N., Basiri, A., Kia, Y., Ali, M.A., Farooq, M., Murugaiyah, V., 2015. A facile ionic liquid promoted synthesis, cholinesterase inhibitory activity and molecular modeling study of novel highly functionalized spiropyrrolidines. *Molecules* 20, 2296–2309.
- Basiri, A., Murugaiyah, V., Osman, H., Kumar, R.S., Kia, Y., Ali, M.A., 2013a. Microwave assisted synthesis, cholinesterase enzymes inhibitory activities and molecular docking studies of new pyridopyrimidine derivatives. *Bioorg. Med. Chem.* 21, 3022–3031.
- Basiri, A., Murugaiyah, V., Osman, H., Kumar, R.S., Kia, Y., Awang, K.B., Ali, M.A., 2013b. An expedient, ionic liquid mediated multi-component synthesis of novel piperidone grafted cholinesterase enzymes inhibitors and their molecular modeling study. *Eur. J. Med. Chem.* 67, 221–229.
- Basiri, A., Murugaiyah, V., Osman, H., Kumar, R.S., Kia, Y., Hooda, A., Parsons, R.B., 2014. Cholinesterase inhibitory activity versus aromatic core multiplicity: a facile green synthesis and molecular docking study of novel piperidone embedded thiazolopyrimidines. *Bioorg. Med. Chem.* 22, 906–916.
- Champagne, P.A., Desroches, J., Hamel, J.D., Vandamme, M., Paquin, J.F., 2015. Monofluorination of organic compounds: 10 years of innovation. *Chem. Rev.* 115, 9073–9174.
- Cummings, J.L., 2004. Alzheimer's disease. *N. Engl. J. Med.* 351, 56–67.
- Genc, H., Kalin, R., Koksak, Z., Sadeghian, N., Kocyigit, U.M., Zengin, M., Gulcin, I., Ozdemir, H., 2016. Discovery of potent carbonic anhydrase and acetylcholinesterase inhibitors: 2-aminoindan β -lactam derivatives. *Int. J. Mol. Sci.* 17, 1736.
- Jasem, Y.A., Thiemann, T., Gano, L., Oliveira, M.C., 2016. Fluorinated steroids and their derivatives. *J. Fluorine Chem.* 185, 48–85.
- Kia, Y., Osman, H., Kumar, R.S., Murugaiyah, V., Basiri, A., Perumal, S., Wahab, H.A., Bing, C.S., 2013a. Synthesis and discovery of novel piperidone-grafted mono- and bis-spirooxindole-hexahydropyrrolizines as potent cholinesterase inhibitors. *Bioorg. Med. Chem.* 21, 1696–1707.
- Kia, Y., Osman, H., Kumar, R.S., Murugaiyah, V., Basiri, A., Perumal, S., Razak, I.A., 2013b. A facile chemo-, regio- and stereoselective synthesis and cholinesterase inhibitory activity of spirooxindole-pyrrolizine-piperidine hybrids. *Bioorg. Med. Chem. Lett.* 23, 2979–2983.
- Kia, Y., Osman, H., Kumar, R.S., Murugaiyah, V., Basiri, A., Khaw, K.Y., Rosli, M.M., 2014a. An efficient ionic liquid mediated synthesis, cholinesterase inhibitory activity and molecular modeling study of novel piperidone embedded α , β -unsaturated ketones. *Med. Chem.* 10, 512–520.
- Kia, Y., Osman, H., Kumar, R.S., Basiri, A., Murugaiyah, V., 2014b. Synthesis and discovery of highly functionalized mono- and bis-spiro-pyrrolidines as potent cholinesterase enzyme inhibitors. *Bioorg. Med. Chem. Lett.* 24, 1815–1819.
- Kia, Y., Osman, H., Kumar, R.S., Basiri, A., Murugaiyah, V., 2014c. Ionic liquid mediated synthesis of mono- and bis-spirooxindole-hexahydropyrrolidines as cholinesterase inhibitors and their molecular docking studies. *Bioorg. Med. Chem.* 22, 1318–1328.
- Kitchen, D.B., Decorez, H., Furr, J.R., Bajorath, J., 2004. Docking and scoring in virtual screening for drug discovery: methods and applications. *Nat. Rev. Drug Disc.* 3, 935–949.

- Kumar, R.S., Almansour, A.I., Arumugam, N., Osman, H., Ali, M.A., Basiri, A., Kia, Y., 2014a. An expedient synthesis and screening for antiacetylcholinesterase activity of piperidine embedded novel pentacyclic cage compounds. *Med. Chem.* 10, 228–236.
- Kumar, R.S., Almansour, A.I., Arumugam, N., Basiri, A., Kia, Y., Kumar, R.R., 2014b. Ionic liquid-promoted synthesis and cholinesterase inhibitory activity of highly functionalized spiropyrrolidines. *Aust. J. Chem.* 68, 863–871.
- Kumar, R.S., Almansour, A.I., Arumugam, N., Althomili, D.M.Q., Altaf, M., Basiri, A., Kotresha, D., Manohar, T.S., Venketesh, S., 2018. Ionic liquid-enabled synthesis, cholinesterase inhibitory activity, and molecular docking study of highly functionalized tetrasubstituted pyrrolidines. *Bioorg. Chem.* 77, 263–268.
- Terry, A.V., Buccafusco, J.J., 2003. The cholinergic hypothesis of age and Alzheimer's disease-related cognitive deficits: recent challenges and their implications for novel drug development. *J. Pharmacol. Exp. Ther.* 306, 821–827.
- Topal, F., Gulcin, I., Dastan, A., Guney, M., 2017. Novel eugenol derivatives: potent acetylcholinesterase and carbonic anhydrase inhibitors. *Int. J. Biol. Macromol.* 94, 845–851.
- Trott, O., Olson, A.J., 2010. AutoDock Vina: improving the speed and accuracy of docking with a new scoring function, efficient optimization, and multithreading. *J. Computational Chem.* 31, 455–461.
- Wang, J., Sanchez-Rosello, M., Acena, J.-L., del Pozo, C., Sorochinsky, A.E., Fustero, S., Soloshonok, V.A., Liu, H., 2014. Fluorine in pharmaceutical industry: fluorine-containing drugs introduced to the market in the last decade (2001–2011). *Chem. Rev.* 114, 2432–2506.
- WHO, 2019. Dementia. Geneva: World Health Organization. Available at: <https://www.who.int/news-room/fact-sheets/detail/dementia> (accessed 15th July 2020).
- WHO, 2017. Global Action Plan on the Public Health Response to Dementia 2017–2025. Geneva: World Health Organization. Available at: http://www.who.int/mental_health/neurology/dementia/action_plan_2017_2025/en/ (accessed 15th July 2020).
- Wilcken, R., Zimmermann, M.O., Lange, A., Joerger, A.C., Boeckler, F.M., 2013. Principles and applications of halogen bonding in medicinal chemistry and chemical biology. *J. Med. Chem.* 56, 1363–1388.
- Zheng, Y.J., Tice, C.M., 2016. The utilization of spirocyclic scaffolds in novel drug discovery. *Expert Opin. Drug Discov.* 11, 831–834.